Advanced Dynamics of Mechanical Systems

Finite Element Method in Structural Dynamics

Assignment 2

Authors:
Gabriele Avi
Enrico Bregni
Francesco Pisacane

Date:
June 17, 2025

Contents

1 Introduction

In this project, we address the dynamic behavior of a mechanical structure inspired by a coal hauling conveyor system, composed of interconnected steel beams of various profiles. The objective is to develop and implement a finite element (FE) model that allows us to investigate the structural response to different load conditions.

In order to perform this, a modal analysis was used. It is a fundamental technique in structural dynamics used to determine the inherent dynamic properties of a structure, namely its natural frequencies (eigenfrequencies) and corresponding vibration patterns (mode shapes). These properties are crucial for understanding a structure's dynamic behavior, predicting its response to dynamic loads (e.g., wind, seismic activity, machinery vibrations), and identifying potential resonance issues.

Project Objectives

The main goals of the project are as follows:

1. **FE Modeling:** develop a finite element model of the structure considering a frequency range up to 20 Hz and applying a safety factor of 2;
2. **Modal Analysis:** determine the first three natural frequencies and corresponding mode shapes. Plot the mode shapes with labels indicating the associated frequencies;
3. **Frequency Response Functions (FRF):** calculate the FRFs relating a vertical force applied at point A to the vertical displacements at points A and B. The excitation spans 0–20 Hz with a resolution of 0.01 Hz;
4. **Modal Superposition:** recalculate the FRFs using only the first two vibration modes. Compare the magnitude and phase diagrams to those from the full model and discuss the differences;
5. **Static Response:** compute the deformation of the structure due to its own weight. Plot the deformed vs. undeformed shapes and quantify the maximum vertical displacement;
6. **Time-Domain Response:** evaluate the vertical displacement at point A caused by a moving load traveling from point B to A at a speed of 2 m/s;
7. **Design Optimization:** propose a structural modification that reduces the maximum static deflection of the free end by 50%, while limiting the increase in structural mass to no more than 20%.

2 Structure definition

The structure under investigation consists of three types of steel beams—IPE 220 (red), IPE 100 (green), and IPE 160 (blue)—with different mass and stiffness properties, distributed along an inclined geometry at 18 degrees.

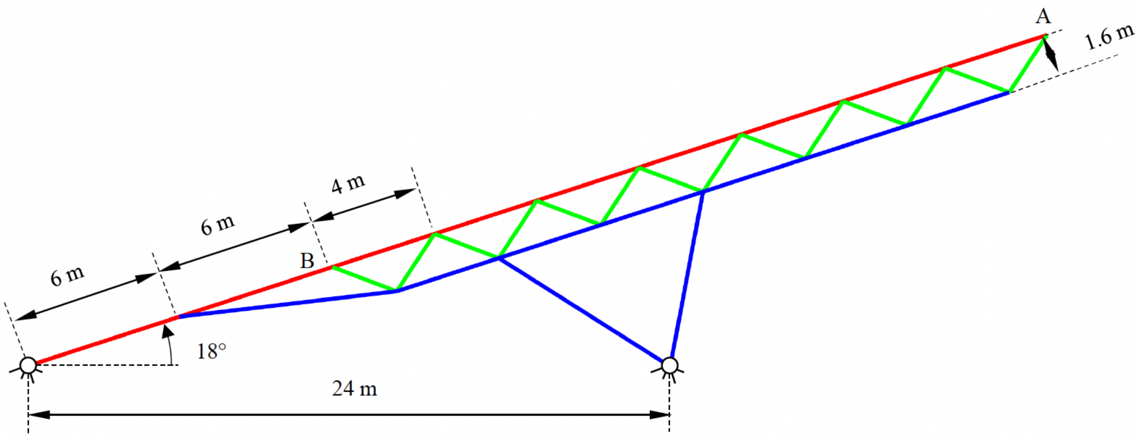

Figure 1: Structure under analysis

The structure is assumed to exhibit *proportional damping*, defined as:

$$\mathbf{C} = \alpha \mathbf{M} + \beta \mathbf{K}$$

where $\alpha = 0.1\,\mathrm{s}^{-1}$ and $\beta = 2 \times 10^{-4}\,\mathrm{s}$.

3 Finite Elements Modeling of the structure

In order to define this structure into the MATLAB code it was necessary to first decide on the mesh. In order to perform a dynamic analysis using linear beam elements, which were designed for static analysis, it is necessary to ensure quasi-static behavior for each element in the structure. This condition can be translated to a maximum allowable length for each element type according to the following formula:

$$L_{max} = \sqrt{\left(\frac{\pi^2}{\eta \Omega_{max}}\right) \cdot \sqrt{\frac{EJ}{m}}}$$

As is possible to notice, the max length depends on different parameters like the max frequency (imposed to 20 Hz) and the properties of the considered beam, which change accordingly with the color as:

Table 1: Beams properties

	M [kg/m]	EA [N]	EJ [Nm^2]
Red beams (IPE 220)	26.2	6.9076E8	5.7380E6
Green beams (IPE 100)	8.1	2.1362E8	3.5400E5
Blue beams (IPE160)	15.8	4.1586E8	1.7995E6

3.1 Elements criteria for dynamic analysis

This will lead to the following different maximum lengths for the 3 beam types:

Table 2: Max length of the elements

Red	Green	Blue
4.2869 m	2.8652 m	3.6404 m

Once these values were obtained, they were chosen 30 nodes and 44 elements (11 red, 14 green and 19 blue). In particular:

- the red elements were divided into 2 lengths: the first 4 elements (connected by nodes 1-2, 2-3, 3-4 and 4-5) are 3 m long, while the others are 4 m long;
- the same for the blue ones, which are 2 m, 2.7 m for the initial 3 elements (connected by nodes 3-27, 27-26 and 26-25) and 3.8 m for the 4 elements near the node 30;
- the green ones instead are all 2.56 m long.

The following figure better explains the division of the structure ad described before:

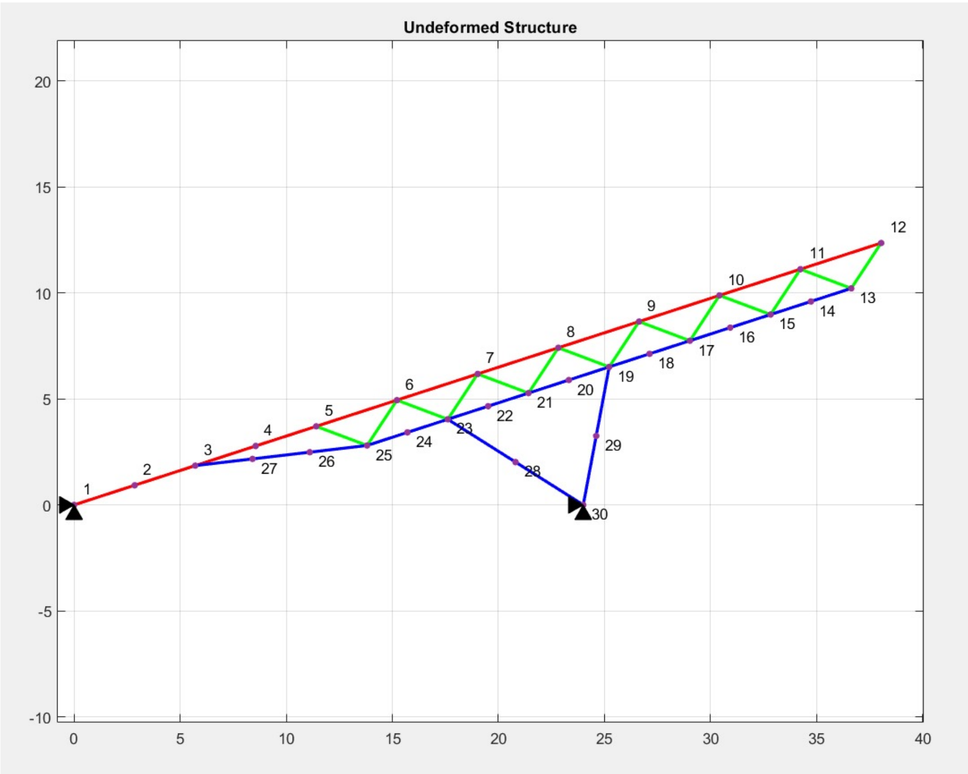

Figure 2: Mesh definition

The structure was implemented in AutoCAD, and from there the coordinates of the nodes were extracted to define the .inp file useful for the successive steps.

4 Computation of natural frequencies and mode shapes

After defining the structure, the modal analysis was made to obtain the eigenfrequencies and the mode shapes. This procedure lies on the assembly of the global mass (M) and stiffness (K) matrices, that can be derived from the energy function formulation (kinetic for the mass matrices and potential for the stiffness ones). For each individual beam element, element-specific mass and stiffness matrices are formulated based on its material properties (EA, EJ, m), and length (l). These element matrices are then assembled into the global system matrices, accounting for the connectivity of elements and the degrees of freedom associated with each node. In this way, everything passes from the local reference system of each element, to the global one, which is the same for all the elements, through a proper matrix rotation.

The script then extracts the free-free mass matrix ($\mathbf{M}_{FF}$) and free-free stiffness matrix ($\mathbf{K}_{FF}$). This step is vital because it isolates the dynamic behavior related only to the free degrees of freedom (DOFs) that are allowed to move or vibrate, excluding any fixed or constrained DOFs. This ensures that the eigenvalue problem focuses on the actual dynamic response of the structure.

With the free-free mass and stiffness matrices established, the natural frequencies and mode shapes were computed by solving the generalized eigenvalue problem:

$$(\omega^2[I] - [M_{FF}]^{-1}[K_{FF}])\mathbf{X} = \mathbf{0}$$

In MATLAB, this is efficiently solved using the $eig(\mathbf{inv}[M_{FF}][K_{FF}])$ function. This operation returns:

- modes: a matrix where each column is an eigenvector, representing a mode shape;
- omega2: a diagonal matrix containing the eigenvalues, which are the square of the natural angular frequencies.

The angular frequencies (ω) were then obtained by taking the square root of the diagonal elements of omega2.

Finally, the 3 natural frequencies with the corresponding mode shapes are founded, and results as reported in the following plots:

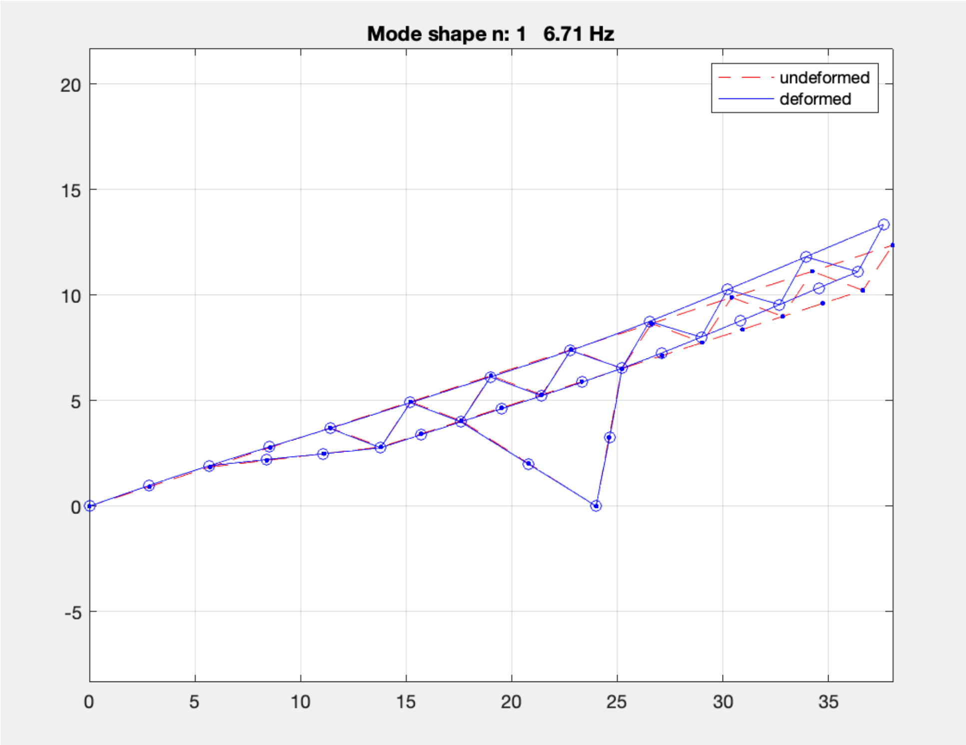

Figure 3: Mode 1 of the structure

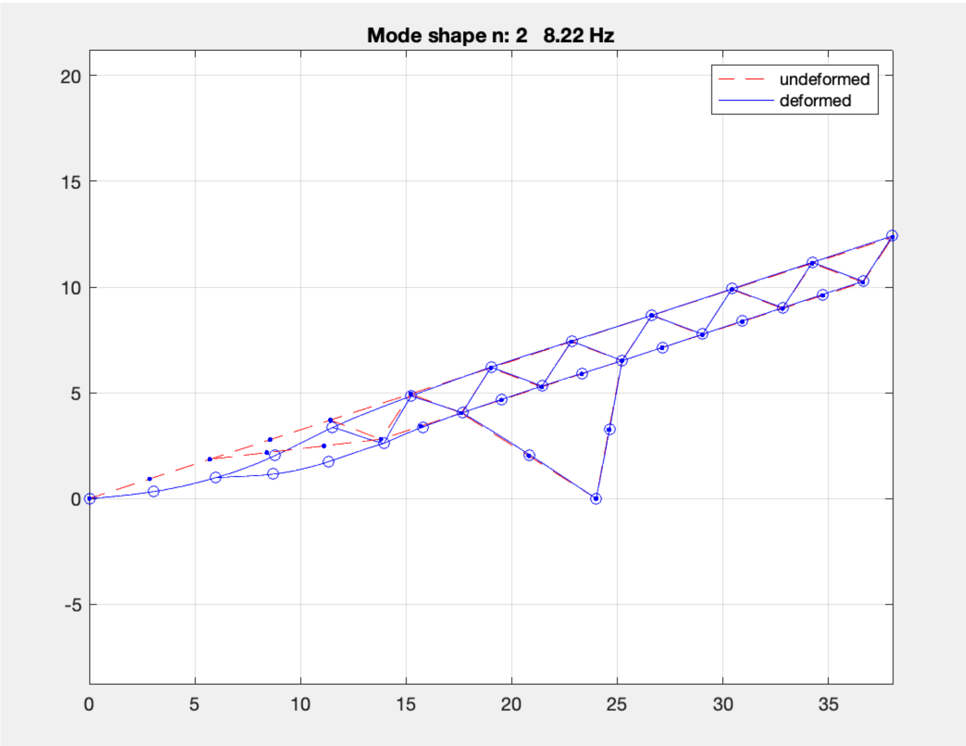

Figure 4: Mode 2 of the structure

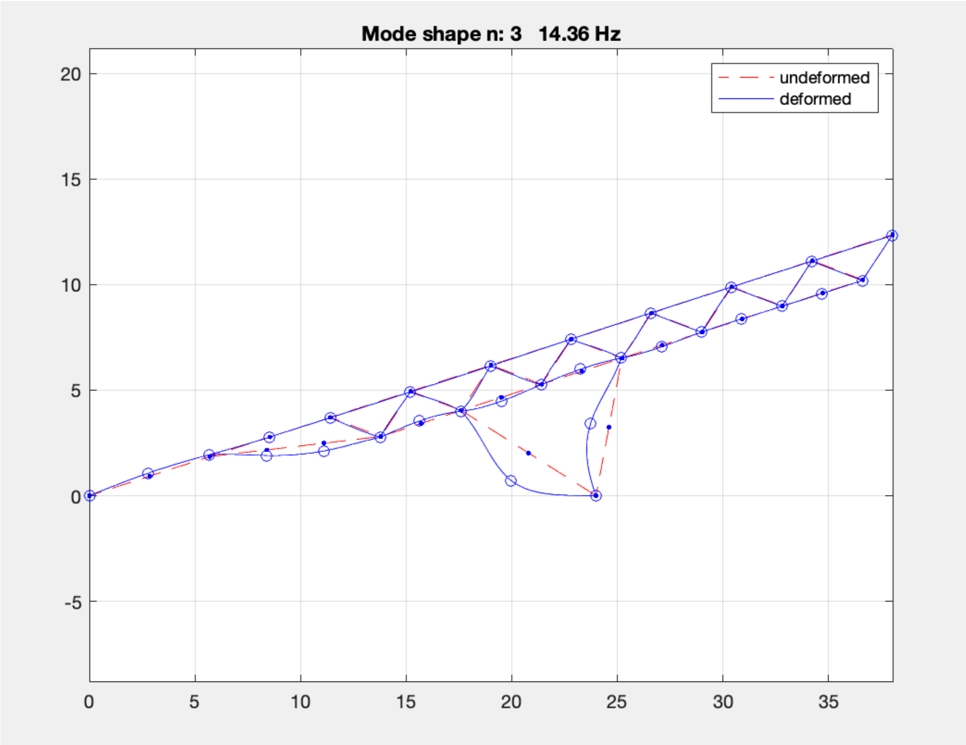

Figure 5: Mode 3 of the structure

The natural frequencies obtained are reported in the following table:

Table 3: Natural Frequencies of the Cantilever Beam (Computed)

mode	Natural freq. [Hz]
1^{st}	6.7118 Hz
2^{nd}	8.2194 Hz
3^{rd}	14.3625 Hz
4^{th}	16.1136 Hz
5^{th}	21.9507 Hz

It is possible to notice that the 5-th mode is at a frequency higher than the Ω_{max}, and so it is out of the quasi-static region, resulting in a wrong representation.

5 Structure Frequency Response Function (using FEM approach)

In this analysis, the Frequency Response Function (FRF) is computed considering an input force applied at position A in the vertical direction, which is assumed to vary between 0-20 Hz with a frequency resolution of 0.01 Hz. The outputs are the vertical displacement at point A and B. So, two FRFs are evaluated:

- **Collocated FRF:** input and output at point A (node 12),
- **Non-collocated FRF:** input at point A, output at point B (node 5).

The procedure to obtain them starts from the dynamic equilibrium equation:

$$[\mathbf{M}_{FF}]\,\ddot{\mathbf{x}}_F + [\mathbf{C}_{FF}]\,\dot{\mathbf{x}}_F + [\mathbf{K}_{FF}]\,\mathbf{x}_F = \mathbf{F}_0 e^{i\Omega t}$$

Assuming a steady-state solution of the form $\mathbf{x}_F = \mathbf{X}_0 e^{i\Omega t}$, we obtain:

$$\mathbf{X}_0 = \left(-\Omega^2\mathbf{M}_{FF} + i\Omega\mathbf{C}_{FF} + \mathbf{K}_{FF}\right)^{-1}\mathbf{F}_0$$

and the Frequency Response Function is defined as:

$$\mathcal{G}(i\Omega) = \left(-\Omega^2\mathbf{M}_{FF} + i\Omega\mathbf{C}_{FF} + \mathbf{K}_{FF}\right)^{-1}$$

The response is then calculated for each frequency using:

$$\mathbf{A}(\omega) = -\omega^2\mathbf{M}_{FF} + i\omega\mathbf{C}_{FF} + \mathbf{K}_{FF}$$

and the displacement vector $\mathbf{X}$ is obtained by solving the following equation, frequency by frequency:

$$\mathbf{X}(\omega) = \mathbf{A}(\omega)^{-1} \cdot \mathbf{F}_0$$

Finally, the magnitude and phase of the FRFs are plotted for a clear visualization of resonance peaks and phase shifts:

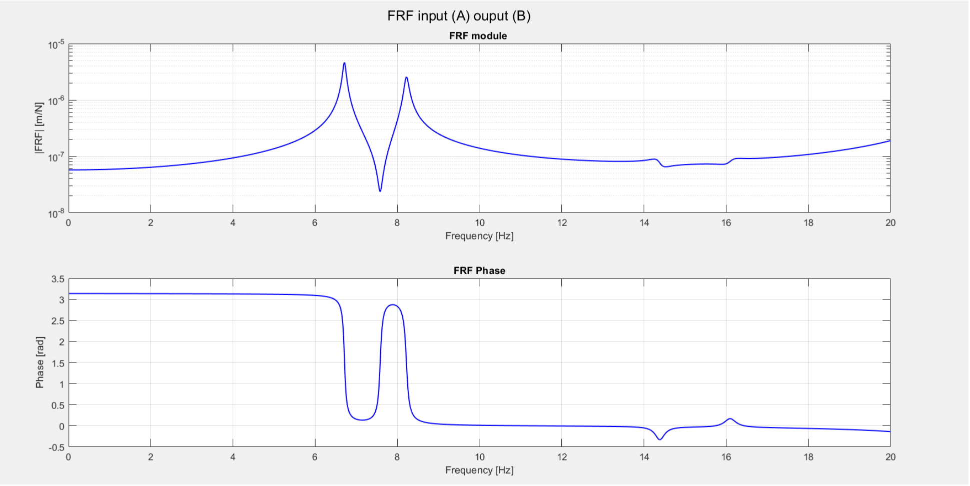

Figure 6: Non-collocated FRF

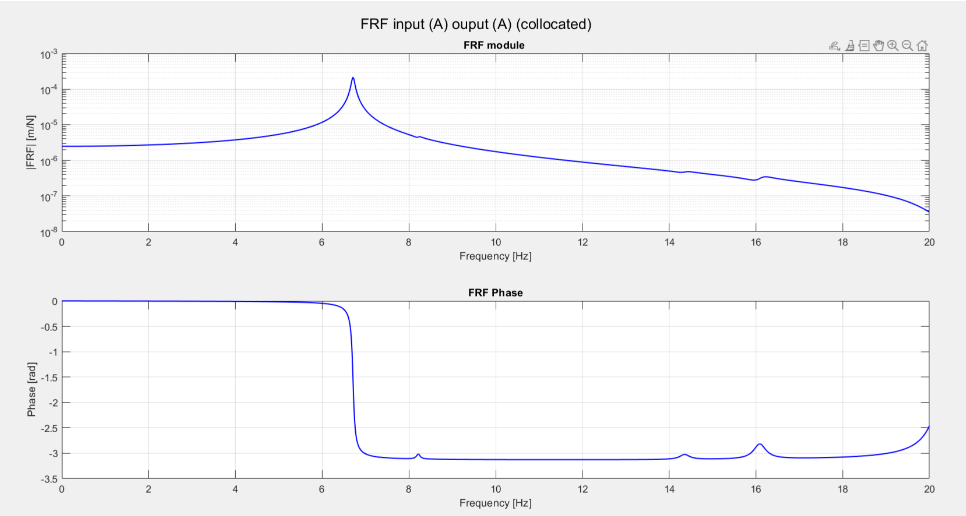

Figure 7: Collocated FRF

The results are consistent with the modal analysis: point A exhibits significant displacement only in the first mode (in the other is almost a node), whereas point B is a node only for mode 3.

6 Comparison between FRF and Modal approach for FRF estimation

In this section, the Frequency Response Function is computed using the modal superposition approach. This method leverages the system's modal properties to efficiently calculate the FRF, especially for systems with a large number of degrees of freedom.

At first, we switched to modal coordinates using the matrix $\mathbf{\Phi}$, where the first two eigenvectors are stacked in columns:

$$[\phi] = [\mathbf{X}^{(1)} \quad \mathbf{X}^{(2)}]$$

This $\mathbf{N} \times \mathbf{2}$ matrix transforms the system's equations from physical to modal coordinates, so we applied it to all the matrices of the system:

- **Mass matrix**:
$$[\mathbf{M_q}] = [\phi]^T[\mathbf{M}][\phi]$$
- **Stiffness matrix**:
$$[\mathbf{K_q}] = [\phi]^T[\mathbf{K}][\phi]$$
- **Damping matrix**:
$$[\mathbf{C_q}] = [\phi]^T[\mathbf{C}][\phi]$$
- **Generalized force vector**:
$$[\mathbf{Q_q}] = [\phi]^T\mathbf{F}$$

These transformed matrices are now diagonal so they form the decoupled equations of motion in the modal domain, which are simpler to solve. In particular, the equation of motion written in principal coordinates results in the following:

$$[\mathbf{M_q}]\{\ddot{\mathbf{q}}\} + [\mathbf{C_q}]\{\dot{\mathbf{q}}\} + [\mathbf{K_q}]\{\mathbf{q}\} = \{\mathbf{Q_q}\}e^{j\Omega t}$$

For each i-th mode, this can be written as:

$$m_{q,ii}\ddot{q}_i + c_{q,ii}\dot{q}_i + k_{q,ii}q_i = Q_{qi}e^{j\Omega t} \quad \text{for } i = 1, 2$$

Assuming a harmonic solution in the form $q_i = q_{0i}e^{j\Omega t}$, we can solve for q_{0i}:

$$q_{0i} = \frac{Q_{qi}}{(-\Omega^2 m_{q,ii} + j\Omega c_{q,ii} + k_{q,ii})} \quad \text{for } i = 1, 2$$

In matrix form, the vector of modal amplitudes $\{\mathbf{q_0}\}$ is given by:

$$\{\mathbf{q_0}\} = \frac{\{\mathbf{Q_q}\}}{(-\Omega^2[\mathbf{M_q}] + j\Omega[\mathbf{C_q}] + [\mathbf{K_q}])}$$

Finally, the nodal displacements in physical coordinates $\{\mathbf{X_0}\}$ are obtained by transforming back from modal coordinates:

$$\{\mathbf{X_0}\} = [\mathbf{\Phi}]\{\mathbf{q_0}\}$$

We can plot and compare the results:

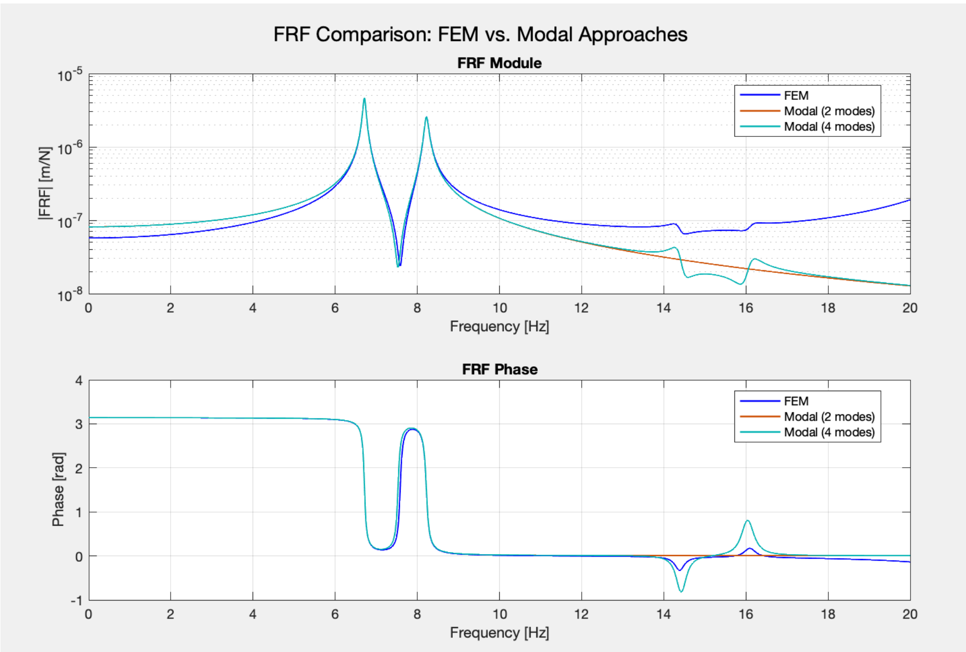

Figure 8: FRF - Modal superposition approach, Non-collocated

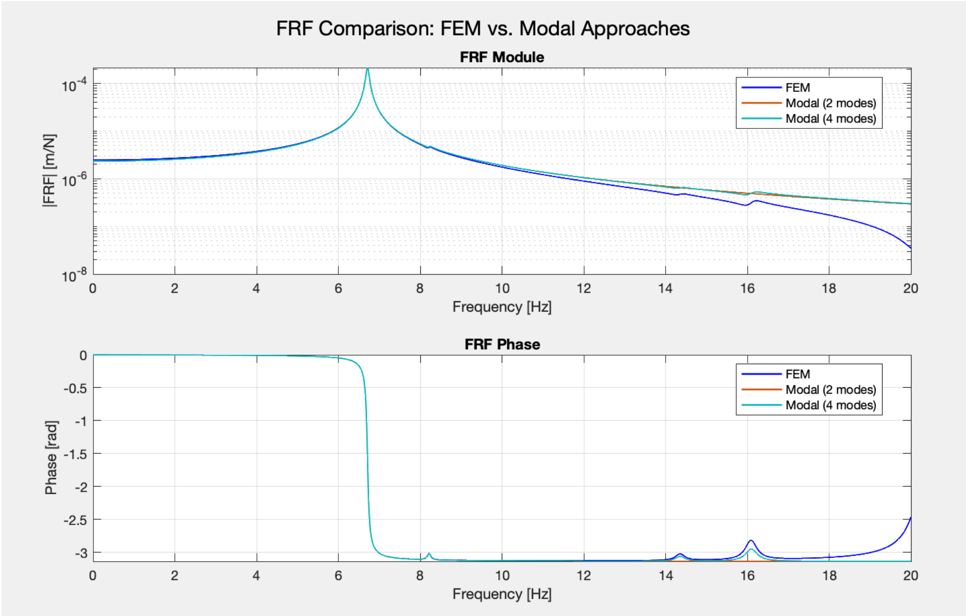

Figure 9: FRF - Modal superposition approach, Collocated

The FRF calculated using the Modal approach yields accurate results within the frequency range encompassing the first two modes. However, at higher frequencies, discrepancies arise due to the influence of additional modes. Nevertheless, the quasi-static region appears to be adequately represented by the modal FRF. Yet, for studies demanding high precision in the system's static response, a greater number of modes should be incorporated, in fact from the plot it is clear that increasing the number of considered modes the FEM result is closer.

7 Static response of structure due to gravitational load

In order to determine the static response of the structure due to its own weight, the load vector needs to be determined. There are various ways to define the load vector; however, the fact that we are in possession of the mass matrix and the gravity load always acts in the vertical direction (global reference system) make for a relatively easy formulation.

- Generate an "acceleration vector" of size (nnod*3) x 1, which is equal to the negative acceleration of gravity in correspondence of every vertical Dof and 0 elsewhere.

$$\{\mathbf{a}\} = \begin{bmatrix} 0 \\ -g \\ 0 \\ \vdots \end{bmatrix}$$

- Multiply the global mass matrix for the acceleration vector to obtain the global load vector.

$$\{\mathbf{F}_g\} = [\mathbf{M}]\{\mathbf{a}\}$$

- Reduce the global load vector to include only the free degrees of freedom. This step is necessary because, in order to solve the finite element system, the stiffness matrix must be reduced to a non-singular form.

$$\{\mathbf{F}_g\} \rightarrow \{\mathbf{F}_{gFF}\}$$

- Solve for the vector of displacements by inverting the stiffness matrix associated to the free Dofs and multiplying it by the free load vector.

$$\{\mathbf{U}\} = [\mathbf{K}_{FF}]^{-1}\{\mathbf{F}_{gFF}\}$$

The resulting static response can be plotted as follows.

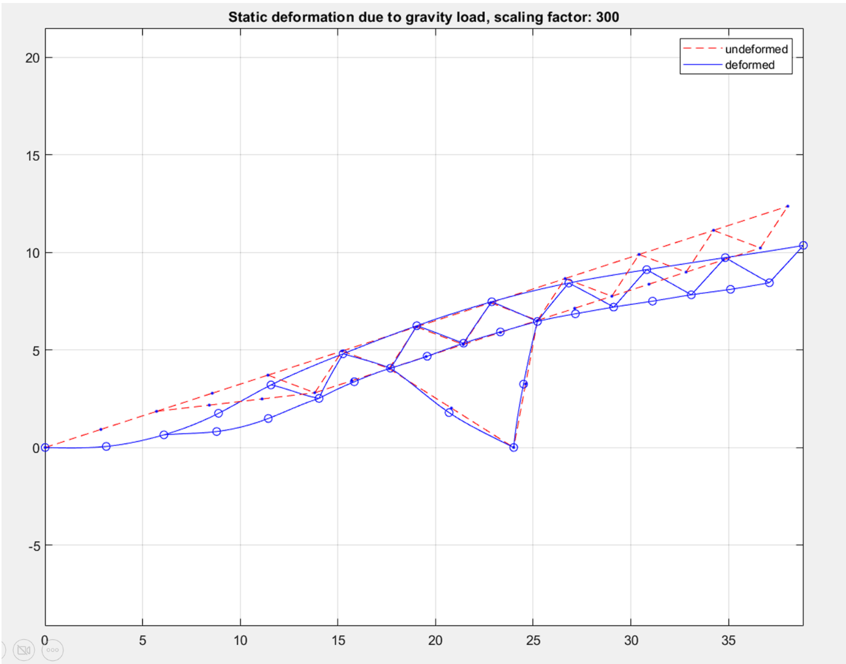

Figure 10: Static deformation of structure under gravitational load

The deformation observable in Figure 10 follows expectation has the greatest deflections are observed far away from the ground constraints, downward deflection of Point A of 6.69 mm, with the left side of the structure behaving similarly to a pin-pin/pin-clamped beam while the right side behaving closer to a cantilever.

8 Time history response due to moving load

This section simulates the dynamic response of the structure under the action of a concentrated moving load. The objective is to compute the time-dependent deformation caused by the mass of a load traveling along a segment of the structure with constant velocity.

Load definition. A portion of the structure (elements 5 to 11) is selected as the path for the moving load. The payload is modeled as a vertical force of constant intensity $F_m = -500\,\mathrm{N}$ (in order to better see the results) moving at a constant velocity $V_M = 2\,\mathrm{m/s}$.

Considering the structural inclination of $\gamma = 18°$, the force is decomposed into local components and expressed in global coordinates through a rotation matrix.

Force computation. At each time step Δt, the load position is incremented by $\Delta x = V_M \cdot \Delta t$. For each position along the element, the nodal equivalent force vector is computed, hence a problem of single force applied in each instant is solved and saved. These vectors are in the local reference system, and they have to be adjusted, bringing them to the global one, using rotation matrix T, and assembled into a global force matrix $F_n(t)_{global}$ representing the time history of the applied load on all DOFs.

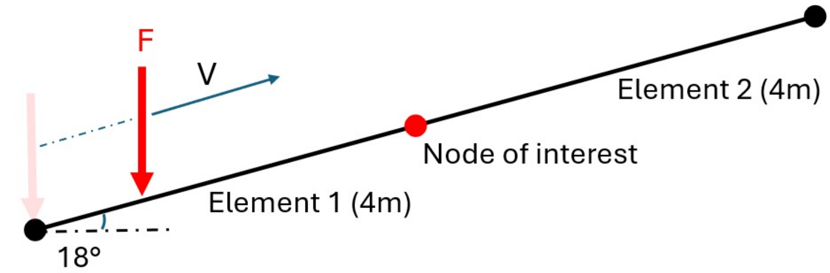

Figure 11: Subsection in global reference system

Note: the "Node of interest" is mentioned as it will later be used for results visualization, but there is no node hierarchy.

$$[T] = \begin{bmatrix} \cos(\gamma) & \sin(\gamma) & 0 & 0 & 0 & 0 \\ -\sin(\gamma) & \cos(\gamma) & 0 & 0 & 0 & 0 \\ 0 & 0 & 1 & 0 & 0 & 0 \\ 0 & 0 & 0 & \cos(\gamma) & \sin(\gamma) & 0 \\ 0 & 0 & 0 & -\sin(\gamma) & \cos(\gamma) & 0 \\ 0 & 0 & 0 & 0 & 0 & 1 \end{bmatrix}$$

Rotation matrix for linear (2 nodes) beam element

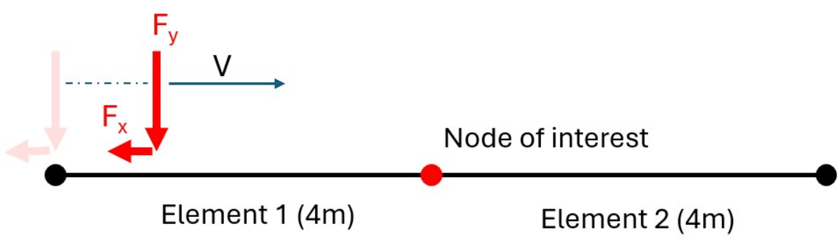

Figure 12: Subsection in local reference system

Load vector calculation. The calculations to compute the equivalent nodal loads of the element over which the load is transitioning, are computed in the local reference system at every time instant. This way a 6x1 local force vector is computed at every time instant. The rotation matrix T, thanks to its orthogonality, can be used to then convert the local force vector into the global reference system.

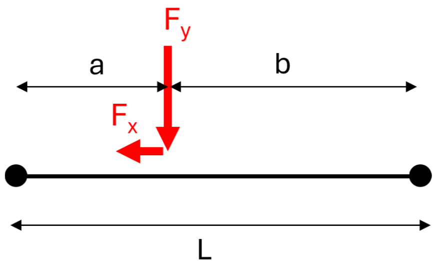

Figure 13: Schematic of load on element in a generic time instant

$$\left\{\mathbf{F}_{\mathrm{n\_element\_local}}\right\} = \begin{bmatrix} \frac{F_x \cdot b}{L} \\ F_y\left(\frac{ab(b-a)}{L^3} + \frac{b}{L}\right) \\ \frac{F_y \cdot ab^2}{L^2} \\ \frac{F_x \cdot a}{L} \\ F_y\left(\frac{ab(a-b)}{L^3} + \frac{a}{L}\right) \\ -\frac{F_y \cdot a^2 b}{L^2} \end{bmatrix}$$

$$\{\mathbf{F}_{\mathrm{n}}\} = [T]^{\mathrm{T}} \left\{\mathbf{F}_{\mathrm{n\_element\_local}}\right\}$$

Load matrix formulation. From here, the load vector still refers to a single element; hence, it is a 6×1 vector. It needs to be scaled to an ndof $\times$ 1 vector with all zeros except at the 6 DOFs associated with the computed loads. All the resulting vectors are appended chronologically to form a load matrix $F_n(t)$ of dimension ndof $\times \left(\frac{\text{time}}{\Delta t}\right)$.

Modal projection and time integration. The global load is projected onto the modal basis using:

$$[Q_n(t)] = [\Phi]^{\mathrm{T}}[F_n(t)]$$

where Φ contains the first n mode shapes. For each mode, the second-order differential equation is solved in time using the `ode45` solver:

$$\ddot{q} + 2\xi\omega\dot{q} + \omega^2 q = \frac{1}{m}Q(t)$$

Response reconstruction. The global structural response is reconstructed by combining modal responses:

$$[X(t)] = [\Phi][q(t)]$$

resulting in the full displacement field over time for all DOFs. X and q are indicated as matrices a the second dimension is time.

8.1 Results visualization.

Load transfer. It is possible to visualize the load transfer of axial force, shear, and bending moment over a node as the load passes. For this we refer to Figure 12 and Figure 11 for the local and global reference respectively. The results are Figure 14 and Figure 15:

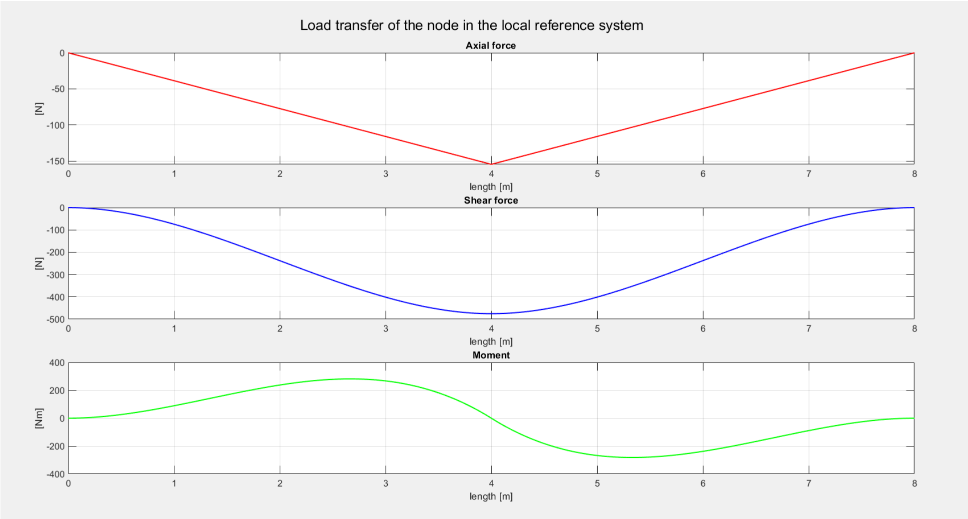

Figure 14: Load transfer of the node in the local system

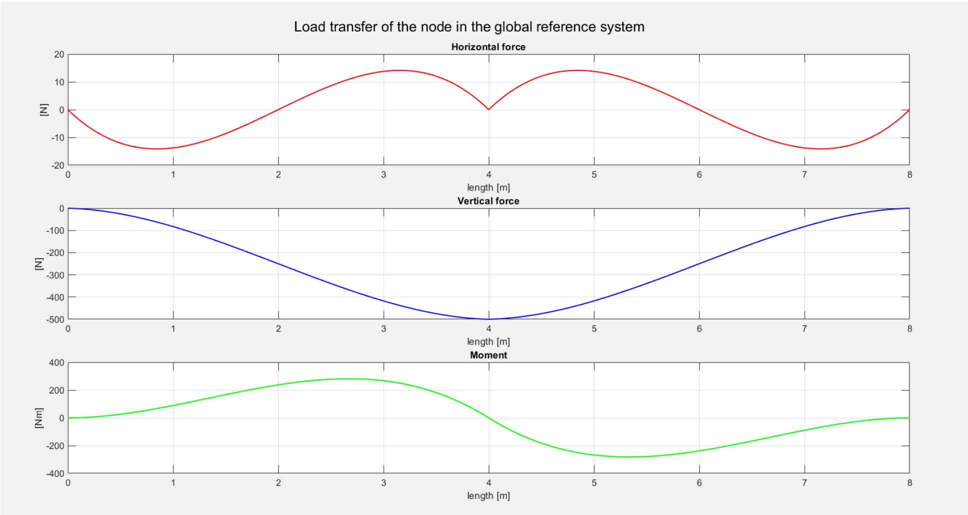

Figure 15: Load transfer of the node in the global system

The load transfer in the local reference frame, Figure 14, follows expectations and physical intuition as the axial force shows a linear behavior with maximum magnitude when the load is directly on top of the node. Similar is the shear but with a non-linear behavior while the moment, also non-linear, is equal to zero when the load is directly over the node.

The load transfer in the global reference frame, Figure 15, ultimately depends on the inclination: 18°. This inclination grants a larger magnitude to the shear force than to the axial one. When these two are projected and combined in the global reference frame, the linear and non-linear behaviors are combined with opposite signs for the horizontal force leading to the noticeably different plot. The opposite is true for the vertical force hence the behavior is similar for both reference frames. The moment load transfer stays unchanged.

Vertical displacement Point A. The vertical displacement of the right extremity of the structure (Point A) is plotted over time, the plot also includes the behavior of the structure after the load falls off:

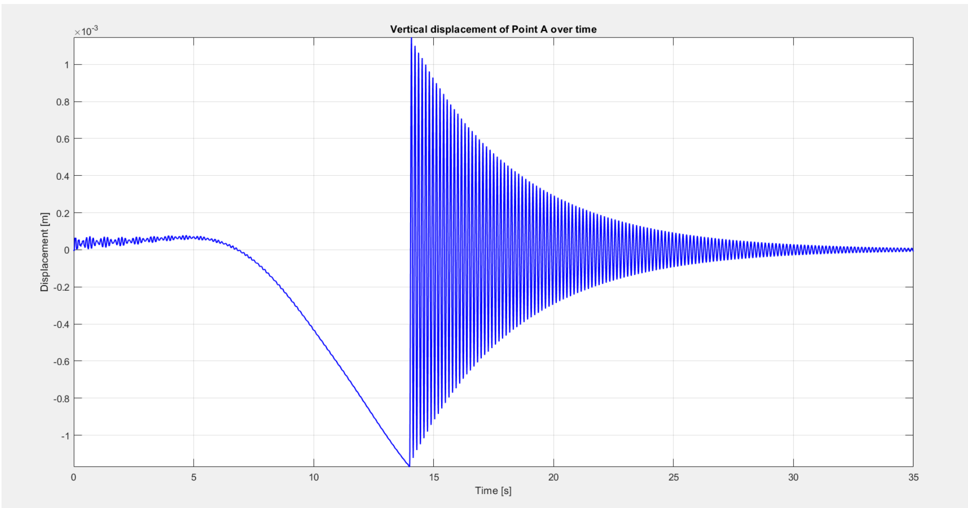

Figure 16: Vibration of the structure apex due to the moving load

Point A has an initial upward deflection due to the left part of the structure being loaded and rotating around the support pin. Afterwards, when the load passes the central pin, the apex starts to deflect downward with a behavior similar to a cantilever beam. Once the load drops from the structure, the latter, is at its maximum displacement and suddenly unloaded. This is equivalent to a SNAP-BACK test and the result is visible as a damped oscillatory motion.

Dynamic response of whole structure. The matrix X(t) contains the dynamic response of all DOFs, not only the vertical displacement of Point A, which we focus on before. Hence it is possible to plot the entire deformation of the structure however since each time instant is a 2D representation, an animation can be used to show the time history of the response. Following, few key frames of the animation:

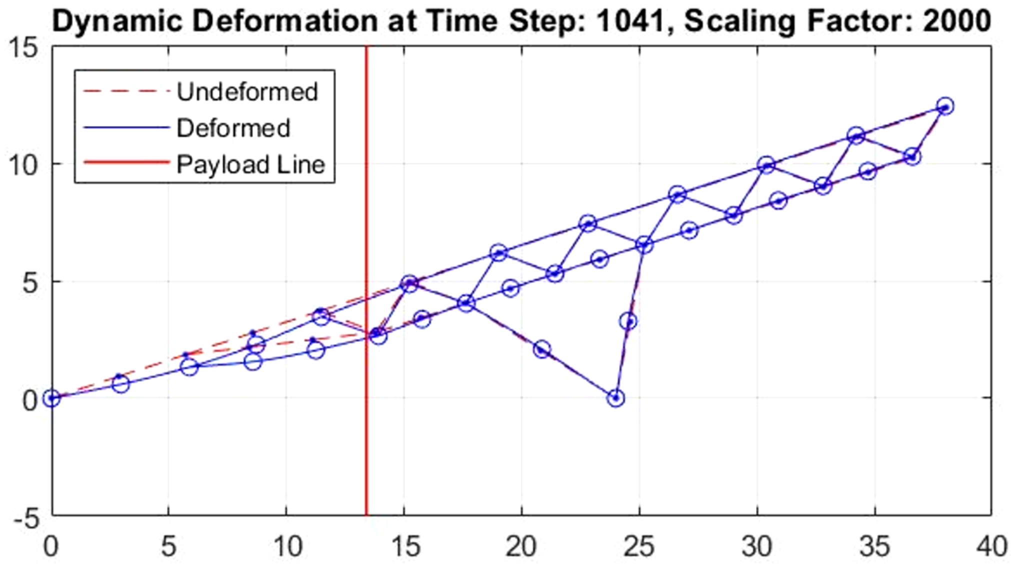

Figure 17: Animation dynamics of whole structure key frame 1

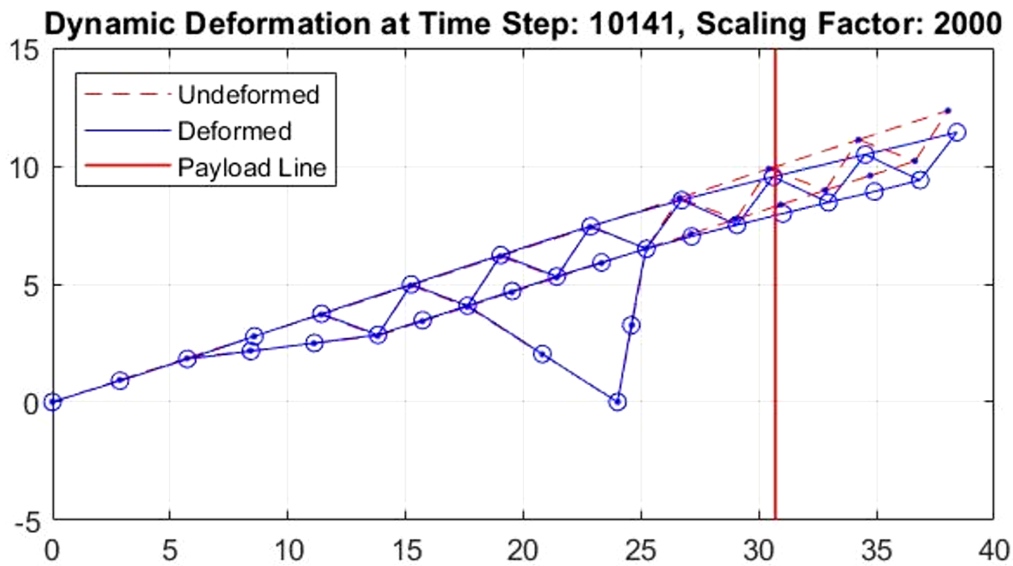

Figure 18: Animation dynamics of whole structure key frame 2

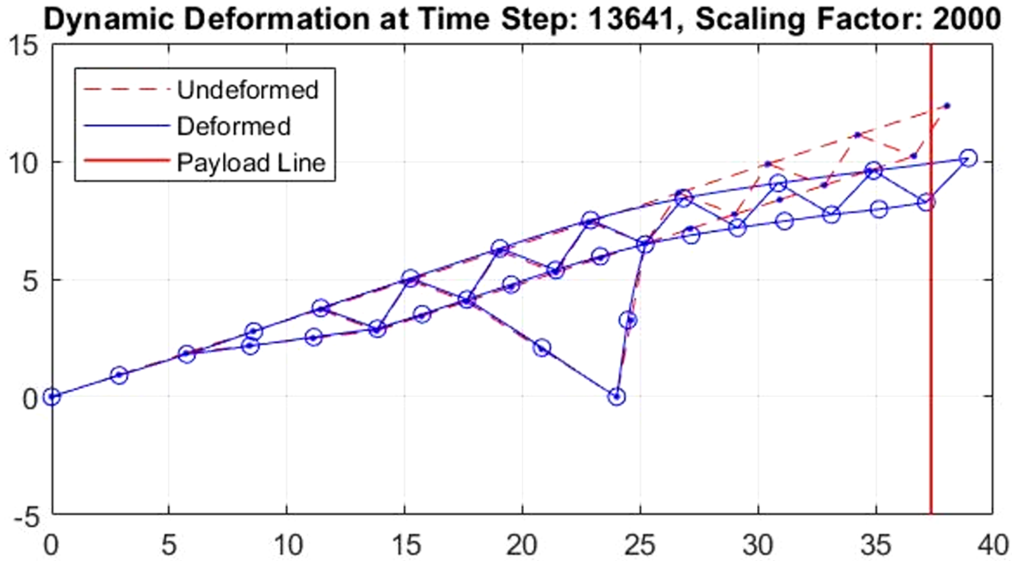

Figure 19: Animation dynamics of whole structure key frame 3

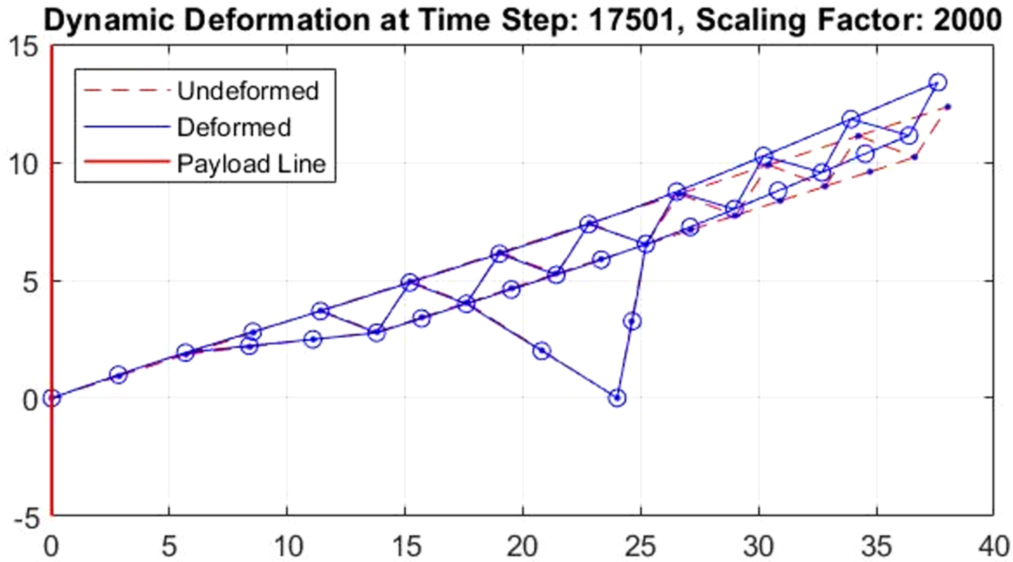

Figure 20: Animation dynamics of whole structure key frame 4

In Figure 17 the load is over the left side of the structure which is being exited. In Figure 18 and Figure 19 the progressive loading of the right side of the structure is observable. Finally, in Figure 20 the response due to the sudden release of the lode can be seen.

9 Structure modification for stiffer static response

The task requires to obtain a stiffer static response under the gravitational load for the vertical deflection of point A (the right most node of the structure). The desired performance is a reduction in vertical deflection of at least 50% with at most a 20% increase in the overall mass of the structure.

The starting is the basic structure, the deflection of which is shown in Section 7 Figure 10. To reduce the vertical deflection at the extremity, a first approach is to add a truss connecting the V-shaped support to the long section acting as a cantilever beam.

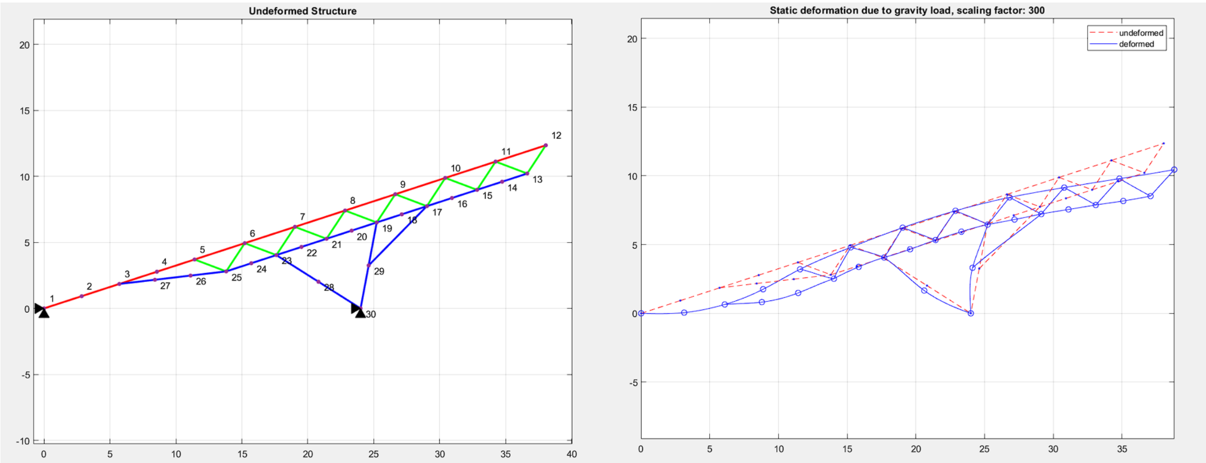

Figure 21: First stiffening attempt, FE model (Right), static deformation (left)

Deflection [mm]	Mass [Kg]	ΔDeflection [%]	ΔMass [%]
-6.35	2170	-5.27	+4.59

Table 4: First stiffening attempt summary table

In Figure 21 it can be seen that the truss alone does not achieve the desired result as the load is transferred to only one of the two beams of the V-shaped support. Since the beam is loaded almost perpendicularly and its center, this leads to compliant response which is reflected in only marginal improvements.

To improve the structure the V-shaped support needs to be stiffened, to do so, three trusses in a triangular pattern can be added and since they are not expected to be loaded significantly, the lightest available beams can be used.

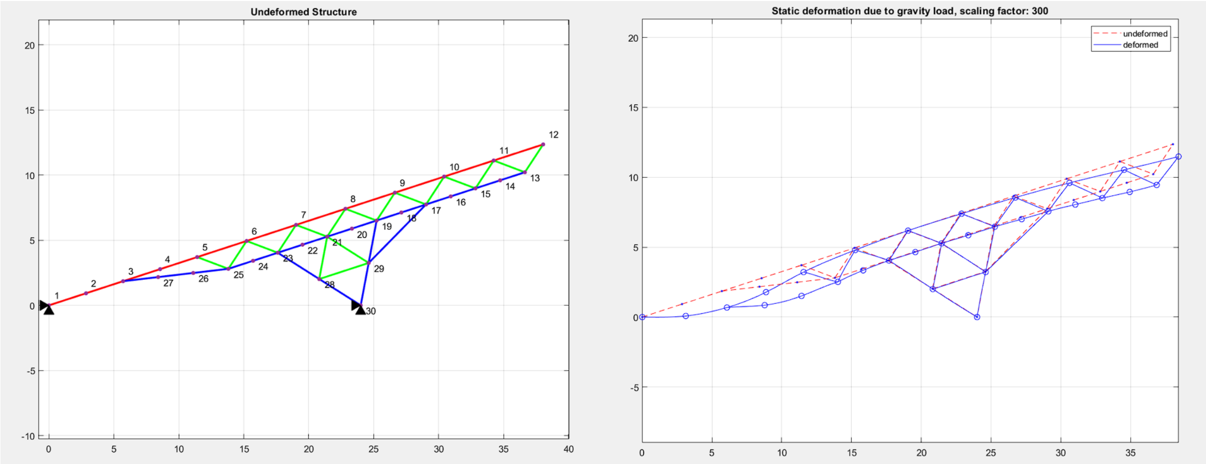

Figure 22: Second stiffening attempt, FE model (Right), static deformation (left)

Deflection [mm]	Mass [Kg]	ΔDeflection [%]	ΔMass [%]
-2.93	2260	-56.20	+8.38

Table 5: Second stiffening attempt summary table

From the deformation shown in Figure 22, it is visible how the V-shaped support results considerably stiffer and this reflects in a great improvement in performances which are summarized in Table 5 far meeting the requirements.

10 Conclusions

This project successfully developed and analyzed a Finite Element model of a steel beam structure, investigating its dynamic and static behaviors.

Modal analysis provided key insights into the structure's natural frequencies and mode shapes, forming the basis for understanding its dynamic response. Comparison of FRFs computed via direct FEM and modal superposition (using two modes) confirmed the modal approach's accuracy in the low-frequency and quasi-static regions. However, it also highlighted its limitations at higher frequencies, where additional modes become crucial. This underscores the balance between computational efficiency and required precision.

The static response to gravitational load was analyzed, showing expected deformations and identifying critical deflection areas.

The moving load analysis enabled a realistic simulation of the structure's response under a traveling concentrated force. Modal projection and time integration highlighted the induced vibrations and the snap-back effect once the load exited the structure. This confirmed the importance of dynamic modeling in capturing transient effects in structural systems.

Finally, the design optimization successfully reduced the maximum static deflection by over 50% with an acceptable mass increase. This was achieved by strategically stiffening the V-shaped support, demonstrating the effectiveness of targeted structural modifications based on a thorough understanding of the system's behavior.

In summary, this project showcased the comprehensive application of FEM in structural dynamics, offering valuable insights for performance prediction and design optimization in engineering applications.

List of Figures

List of Tables